Production of $D^{*\pm}(2010)$ Mesons in DIS Diffractive Interactions at HERA

P. Thompson[a]

[a]School of Physics and Astronomy, University of Birmingham,
BIRMINGHAM B15 2TT, U.K.

The production of diffractive open charm in DIS at HERA probes the gluonic content of the pomeron. The measured cross section $\sigma(ep \to e(D^{*\pm}X)Y)$ is presented differentially as a function of observables exploring the dynamics of the process. The results are compared with a model based on a partonic pomeron as determined in a QCD analysis of the diffractive structure function, with perturbative QCD calculations of two gluon exchange, with a semi-classical model and with a soft colour interaction model.

1. Introduction

Large rapidity gap events observed at HERA constitute approximately 10% of the inclusive deep inelastic scattering (DIS) cross section [1,2]. They are attributed dominantly to pomeron exchange. The rate and kinematic distributions of diffractive open charm production in DIS are sensitive to the gluon content of the exchange, since charm quarks are predominantly produced by the boson-gluon fusion process (BGF). This paper presents a measurement of differential distributions which explore the dynamics of diffractive charm production. Different theoretical approaches to diffractive charm production exist and are discussed below.

1.1. Resolved Pomeron Model

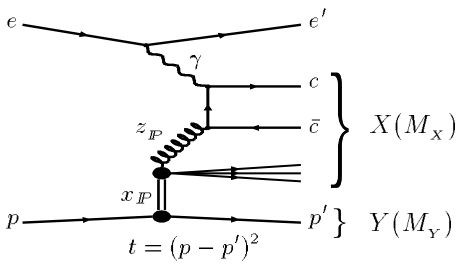

Figure 1. Boson–gluon fusion in the resolved pomeron process. $z_{I\!P}$ denotes the fraction of the pomeron momentum carried by the gluon.

The resolved pomeron model [3] is a partonic interpretation of a factorisable pomeron. The calculation of the cross section factorises into matrix elements based on the parton density of the pomeron and a pomeron flux factor, describing the probability for finding a pomeron in the proton. The pomeron flux is motivated by Regge theory and is approximately proportional to $(1/x_{I\!P})^{1+2\varepsilon}$, where $x_{I\!P}$ is the fraction of the proton's momentum carried by the pomeron and ε is small. Within this picture, the partonic content of the pomeron has been determined by the H1 experiment within a QCD analysis of the inclusive diffractive structure function $F_2^{D(3)}(\beta, Q^2, x_{I\!P})$ [1], where β is the fraction of the momentum of the pomeron carried by the quark interacting with the photon. The parton distributions, obtained from the fit to the data, contain a dominant gluon distribution. Similar gluon-dominated parton distributions have been obtained by Alvero et al. (ACTW) from a range of ZEUS and H1 results [4]. Open charm is produced in the resolved pomeron model by BGF (see figure 1), where the photon, radiated by the incoming lepton, interacts with a gluon of the pomeron, carrying a fraction $z_{I\!P}$ of the pomeron momentum.

1.2. A Two Gluon Exchange Model

Complementary to the approach based on pomeron parton distributions, diffractive $\gamma^* p$ interactions are also modelled in terms of the elastic scattering from the proton of partonic fluctuations of the photon. In the rest frame of the proton, the photon fluctuates a long time before the interaction into a Fock state with a definite parton content ($q\bar{q}$, $q\bar{q}g$, ...), and this partonic state scatters diffractively of the proton. In perturbative QCD diffractive open charm production can be realised by the exchange of two perturbative gluons [5–7]. Assuming such a perturbative approach is valid the cross section for the lowest order process $\gamma^* + p \rightarrow c\bar{c} + p'$ is approximately proportional to the gluon density squared $[x_{I\!P} G_p(x_{I\!P}, \mu)]^2$ of the proton, where μ is the factorisation scale. A calculation based on this approach is implemented in the Monte Carlo generator RAPGAP 2.06 [8]. For a full description $c\bar{c}g$ and higher order Fock states are required. The contribution of the higher order process $\gamma^* + p \rightarrow c\bar{c}g + p'$ to the cross section has been estimated by Ryskin et al [9]. This contribution, in addition to the lowest order process, is implemented in the RIDI [10] Monte Carlo program.

1.3. A Semi-Classical Model

Fluctuations of the photon are also considered in the semi-classical model of Buchmüller, Hebecker and McDermott (BHM) [11]. In this picture, the interaction of the partons from the photon with the proton is described by the superposition of colour fields of the proton according to a simple non-perturbative model that averages over all colour field configurations. The dominant Fock state for charm production in this model is $|c\bar{c}g>$. The model is also implemented in the RAPGAP Monte Carlo program.

1.4. A Soft Colour Interaction Model

In the soft colour interaction model (SCI) [12] the $c\bar{c}$ pair is produced via BGF from the gluon distribution of the proton. With a certain probability the colour structure of the partonic final state is changed during the fragmentation phase, as soft gluon exchanges take place between the outgoing charm quarks and the proton remnant. Large rapidity gap events can be produced when the soft interactions lead to net colour-singlet exchange. The probability for SCI is a free parameter in this model, which has been implemented in the Monte Carlo generator AROMA 2.2 [13].

2. Event Selection

The analyses presented here use data samples from the H1 and ZEUS Collaborations taken during the 1995-1997 running periods where the HERA accelerator collided 820 GeV protons with 27.5 GeV positrons. The standard reconstruction methods of the H1 [14] and ZEUS experiments [15] are used to identify DIS events which contain a $D^{*\pm}$ candidate that decayed through either of the following channels

$$D^{*+} \rightarrow D^0\pi^+ \rightarrow (K^-\pi^+)\pi^+ + (\ c.c.) \quad (1)$$
$$D^{*+} \rightarrow D^0\pi^+ \rightarrow (K^-\pi^+\pi^-\pi^+)\pi^+ + (\ c.c.) \quad (2)$$

The overall branching fraction for the decay channel 1 ('3-prong') and decay channel 2 ('5-prong') is 2.6% and 5.4% respectively [16]. Cuts on the particle track quantities are applied to guarantee a reliable measurement, but these limit the region of phase space measured in the transverse momentum, P_T, and pseudorapidity[1], η, of the $D^{*\pm}$ meson. The measurement of the scattered positron in the main detector is used to reconstruct the DIS kinematics defined in terms of the negative square of the four-momentum transfer at the leptonic vertex, Q^2, and the fractional energy transfer from the positron to the hadronic system in the proton rest frame, y.

From these events, a sample of diffractive events is obtained on the basis of a large gap in the pseudorapidity distribution of final state hadrons adjacent to the leading proton. The rapidity gap is measured using the quantity η_{max}, which is the pseudorapidity of the most forward cluster in the main calorimeter with energy above some specified noise level (of the order 0.3 GeV). The H1 collaboration apply a cut of $\eta_{max} < 3.3$ combined with an absence of any signal in detectors situated in the forward part of the H1 apparatus, which have acceptance at large pseudorapidities. This requirement restricts the mass of the dissociating system M_Y ($M_Y < 1.6$ GeV) and the momentum transfer to the proton t ($|t| < 1$ GeV^2). The ZEUS collaboration apply the cut $\eta_{max} < 1.5$ for the 3-prong decay channel and the

[1]Pseudorapidity is defined to be $-\ln(\tan(\theta/2))$, where θ is the polar angle measured with respect to the proton beam direction.

cut $\eta_{max} < 2.0$ for the 5-prong decay channel. The ZEUS method of selecting diffractive photon dissociative events selects a sample containing little non-diffractive background, but suffers from a significant background contribution from proton dissociative events. This has been estimated from inclusive diffractive ZEUS measurements to be $31 \pm 15\%$ [2]. The value of the η_{max} cut determines the range in $x_{\mathbb{P}}$ for the which the cross section is measured.

3. Total Diffractive $D^{*\pm}$ Cross Section Measurements

3.1. The 3-prong decay channel

The total diffractive $D^{*\pm}$ cross section determined from the 3-prong decay channel is extracted from the full 1995–1997 data sets which correspond to an integrated luminosity of 20.8 pb^{-1} and 43.3 pb^{-1} for the H1 and ZEUS experiments respectively. The kinematic range of the measurement for both experiments is shown in table 1. When t is neglected $x_{\mathbb{P}} = \frac{Q^2+M_X^2}{Q^2+W^2}$ where M_X is the invariant mass of the final state X into which the photon dissociates and W^2 is the square of the hadronic centre of mass energy. Similarly, in this approximation, $\beta = \frac{Q^2}{Q^2+W^2}$.

H1	ZEUS
$2 < Q^2 < 100$ GeV^2	$3 < Q^2 < 150$ GeV^2
$0.05 < y < 0.7$	$0.02 < y < 0.7$
$p_T(D^{*\pm}) > 2$ GeV	$p_T(D^{*\pm}) > 1.5$ GeV
$\lvert\eta(D^{*\pm})\rvert < 1.5$	$\lvert\eta(D^{*\pm})\rvert < 1.5$
$x_{\mathbb{P}} < 0.04$	$0.002 < x_{\mathbb{P}} < 0.012$
–	$\beta < 0.8$
$M_Y < 1.6$ GeV	$M_Y = m_p$
$\lvert t\rvert < 1$ GeV^2	–

Table 1
The kinematic ranges of the H1 and ZEUS diffractive $D^{*\pm}$ measurements for the 3-prong decay channel.

After applying the kinematic cuts listed above, the number of $D^{*\pm}$ mesons extracted from a fit to the invariant mass difference distribution $\Delta M = M(K^-\pi^+\pi^+) - M(K^-\pi^+)$ was measured to be $38 \pm 10(stat.) \pm 4(syst.)$ for the H1 experiment and 59 ± 9 for the ZEUS experiment. These data were then corrected for the acceptance of the detector using Monte Carlo events generated using RAPGAP, running in the resolved pomeron mode, which gives a reasonable description of the data. The cross sections for diffractive $D^{*\pm}$ production in the kinematic region above were measured to be $\sigma(ep \to e(D^{*\pm}X)Y) = (154 \pm 40 \pm 35)$pb (H1 preliminary [17]) and $\sigma(ep \to e(D^{*\pm}X)Y) = (379 \pm 66^{+99}_{-140})$pb (ZEUS preliminary [18]), where the first errors are statistical and the second systematic. Comparisons between the two cross sections are difficult due to the different kinematic regions covered. However, using the Monte Carlo models to interpolate between the two kinematic regions suggests that the cross sections are in disagreement at the level of approximately 2σ.

3.2. The 5-prong decay channel

The ZEUS collaboration have also measured the diffractive $D^{*\pm}$ cross section using the 5-prong decay channel within the 1996-1997 dataset which corresponds to an integrated luminosity of 37 pb^{-1}. The cross section is measured in the kinematic range $1 < Q^2 < 480$ GeV^2, $0.04 < y < 0.7$, $2 < p_T(D^{*\pm}) < 9$ GeV, $|\eta(D^{*\pm})| < 1.5$, $x_{\mathbb{P}} < 0.015$ and $\beta < 0.8$. Here the $D^{*\pm}$ signal was found to contain 121 ± 24 events corresponding to a cross section of $\sigma(ep \to e(D^{*\pm}X)Y) = (526 \pm 110^{+200}_{-240})$pb (ZEUS preliminary [19]). The kinematic regions defined for the two ZEUS measurements are substantially different. In order to make a direct comparison the 5-prong measurement may be interpolated to the kinematic region described in section 3.1 using the Monte Carlo simulation employed for the cross section unfolding. The result of this interpolation is found to be $\sigma(ep \to e(D^{*\pm}X)Y) = (398 \pm 83^{+154}_{-180})$pb which is in excellent agreement with the result from the 3-prong decay channel.

4. Differential Cross Sections

The differential diffractive cross sections for the H1 experiment are shown in figures 2 and 3 and for the ZEUS experiment in figures 4 and 5. In figure 2 the cross section is shown as a function

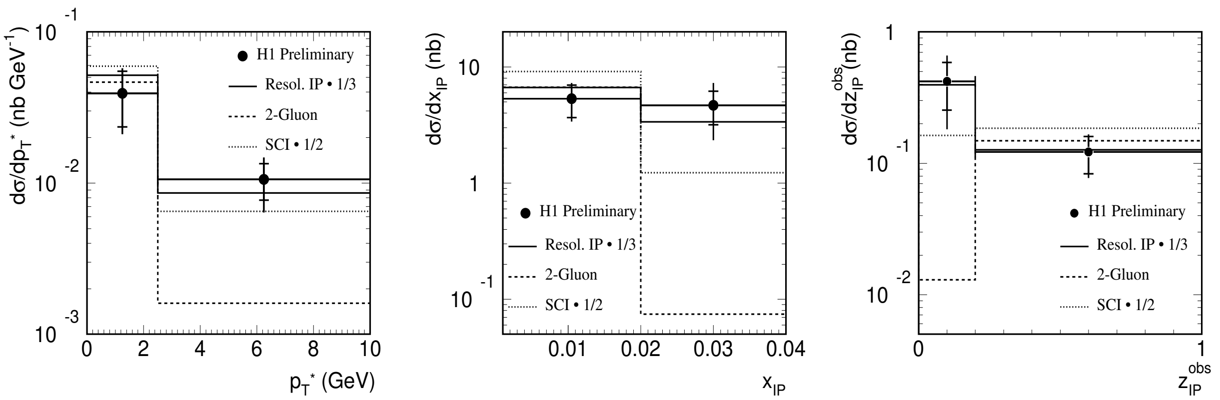

Figure 2. *Cross sections $\sigma(ep \to e(D^{*\pm}X)Y)$ measured by the H1 experiment as a function of p_T^*, where p_T^* denotes the transverse momentum of the $D^{*\pm}$ in the γ^*p centre of mass system, the fraction $x_{I\!P}$ of the proton momentum carried by the pomeron and $z_{I\!P}^{obs}$, which is an approximation to the momentum fraction of the pomeron carried by the gluon entering the hard interaction. The data are points with error bars (inner: statistical, outer: total) and are compared with the resolved pomeron model (solid line), the 2–gluon model for the process $\gamma^* + p \to c\bar{c} + p'$ [6] (dashed line) and the SCI–model (dotted line). The resolved pomeron model is normalised by a factor of $1/3$ and the SCI model by a factor of $1/2$.*

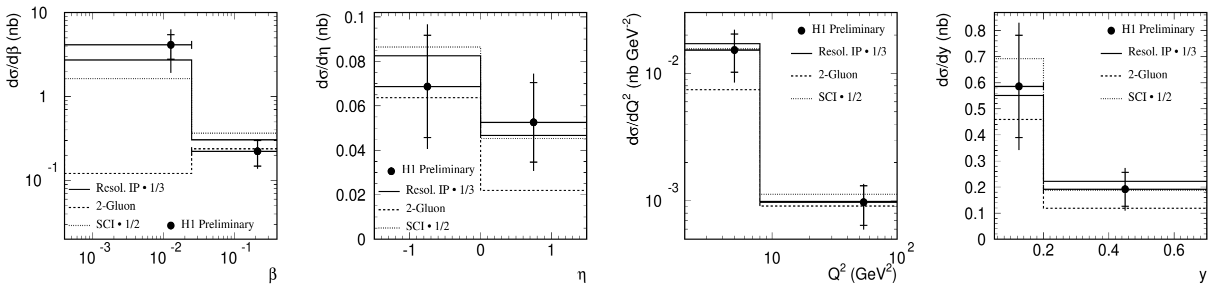

Figure 3. *Cross sections $\sigma(ep \to e(D^{*\pm}X)Y)$ measured by the H1 experiment as a function of β, η, Q^2 and y. The data are points with error bars (inner: statistical, outer: total).*

of the transverse momentum of the D^* in the γ^*p centre of mass system p_T^*, of $x_{I\!P}$, and of the hadronic observable $z_{I\!P}^{obs}$, which is an approximation (in the resolved pomeron picture) to the momentum fraction of the pomeron carried by the interacting gluon. $z_{I\!P}$ is given by

$$z_{I\!P} = \beta \cdot \left(1 + \frac{\hat{s}}{Q^2}\right) = \frac{M_{c\bar{c}}^2 + Q^2}{M_X^2 + Q^2},$$

where $M_{c\bar{c}}$ can be reconstructed using the scattered positron and the tagged $D^{*\pm}$ meson (see also [14]). If the partons could be observed directly, in the perturbative two gluon model for $c\bar{c}$ fluctuations of the photon $z_{I\!P} = 1$ would always hold. In figure 3 cross sections are also shown as a function of β, η, Q^2 and y. The resolved pomeron approach reproduces well the shape of the spectra and in particular the fact that the data show a sizeable fraction of "resolved" pomeron production in the low $z_{I\!P}^{obs}$ region. However, the model fails in the overall normalisation by a factor of 2 to 3. The two gluon model for $c\bar{c}$ fluctuations of the photon, on the other hand, does not describe the regions of higher masses M_X i.e. low $M_{c\bar{c}}/M_X$, low $z_{I\!P}^{obs}$. It is apparent, also from the p_T^* distribution, that higher order contributions such as $\gamma^* + p \to c\bar{c}g + p'$ are needed. (The discrepancy at low β reflects the behaviour at high $x_{I\!P}$.) It is, however, interesting to note that the data in regions where the hadronic system X predominantly consists of the $c\bar{c}$ system alone (high

$z_{I\!P}^{obs}$) are well reproduced in magnitude. The SCI model fails in the overall normalisation by a factor of about 2 although it produces reasonably well the shape of the differential distributions within the large errors.

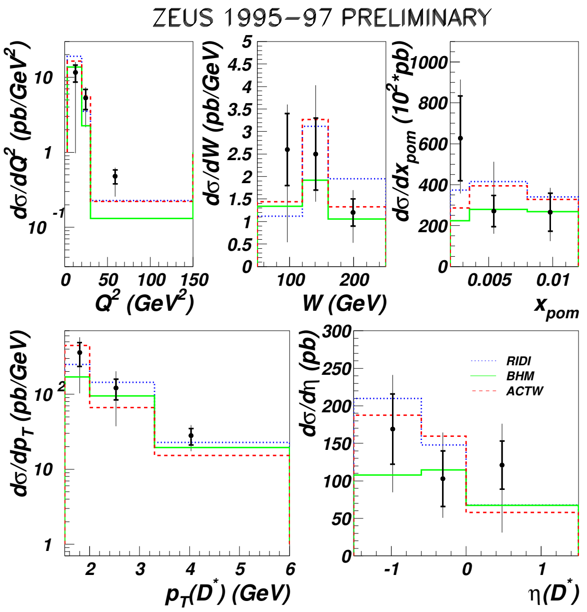

Figure 4. *The differential cross sections measured by the ZEUS experiment from the 3-prong decay channel versus Q^2, W, $x_{I\!P}$, $p_T(D^{*\pm})$ and $\eta(D^{*\pm})$. The data are points with error bars (inner: statistical, outer: total) and are compared with the the RIDI Monte Carlo program (dotted line), the semi-classical model of BHM (solid line) and the resolved pomeron model of ACTW (dashed line).*

The ZEUS experiment have measured the differential $D^{*\pm}$ cross sections from both decay channels as a function of Q^2, W, $x_{I\!P}$, $p_T(D^{*\pm})$ and $\eta(D^{*\pm})$. The results are shown in figures 4 and 5. In each plot the results are compared with three different theoretical predictions. The solid line indicates the prediction of the semi-classical model of BHM, while the dashed line indicates the predictions made by Alvero et al (ACTW). Finally, the dotted line shows predictions of the Ryskin pQCD model as implemented

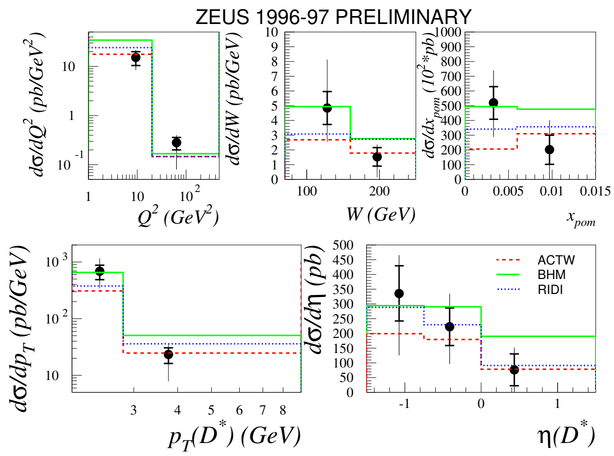

Figure 5. *The differential cross sections measured by the ZEUS experiment from the 5-prong decay channel versus Q^2, W, $x_{I\!P}$, $p_T(D^{*\pm})$ and $\eta(D^{*\pm})$. The data are points with error bars (inner: statistical, outer: total) and are compared with the the RIDI Monte Carlo program (dotted line), the semi-classical model of BHM (solid line) and the resolved pomeron model of ACTW (dashed line).*

in the RIDI Monte Carlo generator. This includes higher order corrections which are known to cause a large normalisation uncertainty in the predictions. For this reason, the predictions from RIDI have been normalised to the data cross section. The agreement in normalisation between the data and the predictions of ACTW are consistent with the data showing a preference for a gluon-dominated pomeron. All three models appear to describe the differential distributions reasonably well, but more statistics are clearly required in order to discriminate between the different models.

The ratio, R, of diffractive $D^{*\pm}$ to total $D^{*\pm}$ production has been measured by the ZEUS experiment from the 5-prong decay channel to be $R = 8.9 \pm 2.4^{+1.7}_{-1.6}\%$ and from the 3-prong decay channel to be $R = 7.0 \pm 1.3^{+1.7}_{-1.8}\%$. These values are in good agreement even though they are measured in different kinematic ranges. They are also consistent with the fraction of the total cross section attributed to diffractive scattering [2]. The dependence of the ratio on W and Q^2 has been measured from the 3-prong decay channel and is shown in figure 6. The ratio is found to be flat within the errors.

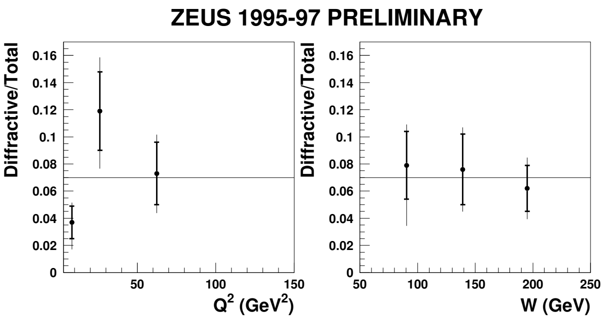

Figure 6. *The ratio of diffractive $D^{*\pm}$ to total $D^{*\pm}$ production as a function of Q^2 and W measured by the ZEUS collaboration from the 3-prong decay channel. The inner error bars represent the statistical error on the data points and the outer error bars represent the statistical and systematic errors added in quadrature. The solid line indicates the average ratio $R = 7.0 \pm 1.3^{+1.7}_{-1.8}\%$.*

5. Conclusions

The dynamics of diffractive charm production have been studied at HERA through the measurement of the total and differential cross section for $D^{*\pm}$ meson production. In the kinematic range probed, the ZEUS experiment measure a cross section which is consistent with the expectation based on the resolved pomeron model with gluon-dominated parton distributions derived from the QCD analysis of inclusive diffractive DIS data. In contrast, the H1 experiment observe a difference of a factor 2-3 in the normalisation between the data and the predictions. The differential cross sections have been measured and compared to several different calculations. The resolved pomeron model is found to describe well the shape of all the differential distributions. The shapes of the distributions indicate that in perturbative two-gluon exchange models the data require higher order contributions to the leading order process $\gamma^* + p \rightarrow c\bar{c} + p'$. The data are reasonably well described in shape by the SCI and semi-classical models.

REFERENCES

1. C. Adloff et al., H1 Coll., Z.Phys. **C76** (1997) 613.
2. J. Breitweg et al., Euro. Phys. J **C6** (1999) 43.
3. G. Ingelmann, P.E. Schlein, Phys. Lett. **B152** (1985) 256; A. Donnachie, P.V. Landshoff, Phys. Lett. **B191** (1987).
4. L. Alvero et al. Phys. Rev. **D59** (1999) 74022; L. Alvero et al. hep-ph/9806340.
5. J. Bartels, H. Lotter, M. Wüsthoff, Phys. Lett. **B 379** (1996) 239.
6. J. Bartels, C. Ewerz, H. Lotter, M. Wüsthoff, *Phys. Lett.* B, **386** (1996) 389.
7. H. Lotter, *Phys. Lett.* B, **406** (1997) 171.
8. H. Jung, *Comput. Phys. Commun.* , **86** (1995) 147.; (for update see http://www-h1.desy.de/ jung/rapgap/rapgap.html)
9. E. M. Levin, A. D. Martin, M. G. Ryskin, T. Tenbner, Z. Phys. **C74** (1997) 671.
10. M. G. Ryskin, Sov. J. Nucl. Phys. **52** (1990) 529; M. G. Ryskin, S. Y. Sivoklokov and A. Solano, Proc. of Int. Conf. on Elastic and Diffractive Scattering, Ed. H. M. Fried et al.,(1993) World Scientific; M. G. Ryskin and A. Solano, Proc. of the Workshop 'Monte Carlo Generators for HERA Physics', Ed. G. Grindhammer et al.,(1999) Hamburg (to be published).
11. W. Buchmüller, A. Hebecker and M. F. McDermott, Phys. Lett. **404** (1997) 353.
12. A. Edin, G. Ingelman, J. Rathsman, *Z. Phys.* C, **75** (1997) 57., *Phys. Rev.* D, **56** (1997) 7317.
13. G. Ingelman, J. Rathsman, G.A. Schuler *Comput. Phys. Commun.* , **101** (1997) 135.
14. H1-Collaboration., S. Adloff et al., *Nucl. Phys.* B, **545** (1999) 21.
15. J. Breitweg et al., Phys. Lett. **407** (1997) 402.
16. C. Caso *et al.* (Particle Data Group), Eur. Phys J. **C3** (1998) 1.
17. H1 Collaboration, Abstract 558, XXIX ICHEP, Vancouver 1998.
18. ZEUS Collaboration, Abstract 785, XXIX ICHEP, Vancouver 1998.
19. ZEUS Collaboration, Abstract 527, EPS HEP, Tampere 1999.